Numerical simulation of light propagation through composite and anisotropic media using supercomputers

Roman Galev[1], Alexey Kudryavtsev[1,2], and Sergey Trashkeev[3,4]

[1] Khristianovich Institute of Theoretical and Applied Mechanics, 630090 Novosibirsk, Russia, galev@itam.nsc.ru, alex@itam.nsc.ru
[2] Novosibirsk State University, 630090 Novosibirsk, Russia
[3] Institute of Laser Physics, 630090 Novosibirsk, Russia, sitrskv@mail.ru
[4] Voevodsky Institute of Chemical Kinetics and Combustion, 630090 Novosibirsk, Russia

Abstract. Laser beam propagation through and absorption in composite and anisotropic media is simulated by solving numerically Maxwell's equations with the FDTD method. Laser treatment of materials, light beam transformation in micron-sized optical fiber systems and liquid crystalline materials, generation of optical vortices (beams with non-zero orbital angular momentum) due to interaction with liquid crystal disclinations are considered. Typical grids used for simulations consist of tens and hundreds of millions of cells. The numerical code is parallelized using geometrical domain decomposition and the MPI library for data transfer between nodes of a computational cluster.

Keywords: computational electromagnetism, FDTD scheme, laser treatment of materials, metamaterials, soft matter, liquid crystals

1 Introduction

The development of coherent sources of optical radiation is often referred to as "optical revolution". Lasers have had a deep impact on telecommunications, industry, medicine, science and everyday life. Today we are witness to a new great progress in optical technologies which is resulted from a substantial body of pure and applied research in material science and soft matter physics. Optical properties of some soft matter materials (such as liquid crystals) can be substantially altered by weak external electromagnetic fields or thermal and mechanical stresses that opens unique opportunities for dynamic control of light propagation. Optical metamaterials, i.e. structured materials engineered to have optical properties that cannot be found in nature, enable us to manipulate radiation by blocking, absorbing, enhancing, or bending electromagnetic waves and achieve benefits that go far beyond what is possible with conventional materials.

Numerical simulation is of great importance for better understanding of complex phenomena connected with light propagation through non-homogeneous, anisotropic and structured media as well as for development of new optical technologies. With the advent of modern supercomputers, numerical simulation of quite complicated optical systems and devices based on direct solving Maxwell's equations has become feasible. In the present paper we describe some examples of numerical simulations of problems connected with laser processing of materials, development of fiber-coupled liquid crystal systems and generation of "optical vortices", i.e. light beams with non-zero orbital angular moment, using liquid crystals.

2 Numerical method and its computer implementation

Maxwell's equations in an anisotropic inhomogeneous medium can be written as

$$\frac{\partial \mathbf{D}}{\partial t} = -\left(\mathbf{J} + \sigma_e \mathbf{E}\right) + \nabla \times \mathbf{H}, \qquad \mathbf{D} = \bar{\bar{\epsilon}}\,\mathbf{E}, \tag{1}$$

$$\frac{\partial \mathbf{B}}{\partial t} = -\left(\mathbf{M} + \sigma_m \mathbf{H}\right) - \nabla \times \mathbf{E}, \qquad \mathbf{B} = \bar{\bar{\mu}}\,\mathbf{H}. \tag{2}$$

Here t is time, $\mathbf{r} = (x, y, z)$ is the vector of spatial coordinates, $\nabla \equiv \partial/\partial \mathbf{r}$, $\mathbf{E}$ and $\mathbf{H}$ are the electric and magnetic fields, $\mathbf{D}$ and $\mathbf{B}$ are the densities of electric and magnetic fluxes, $\mathbf{J}$ and $\mathbf{M}$ are the densities of external electric and magnetic currents, $\bar{\bar{\epsilon}}$ and $\bar{\bar{\mu}}$ are the tensors of electrical permittivity and magnetic permeability, σ_e and σ_m are the electric and magnetic conductivities. In our simulations we consider nonmagnetic materials so that $\bar{\bar{\mu}}$ is the identity tensor and $\mathbf{B} \equiv \mathbf{H}$. The magnetic conductivity σ_m does not vanish only in a buffer zone surrounding the computational domain (see below). The electric conductivity σ_e and the positive definite symmetric tensor $\bar{\bar{\epsilon}}$ are assumed to be functions of $\mathbf{r}$.

Equations (1,2) are solved numerically with the FDTD (Finite-Difference Time-Domain) method [1, 2]. The FDTD is a simple but smartly devised and efficient second-order scheme that utilizes a computational grid staggered both in space and time so that electrical and magnetic fields are calculated in alternating time moments and all field components are determined in different points of the computational stencil — see Fig. 1. The FDTD scheme for x-components of Eqs. (1,2) reads as

$$\begin{aligned} \frac{D_x\big|^{n+1/2}_{i,j',k'} - D_x\big|^{n-1/2}_{i,j',k'}}{\Delta t} = \frac{H_z\big|^{n}_{i,j'',k'} - H_z\big|^{n}_{i,j,k'}}{\Delta y} - \frac{H_y\big|^{n}_{i,j',k''} - H_y\big|^{n}_{i,j',k}}{\Delta z} - \\ J_x\big|^{n}_{i,j',k'} - \frac{1}{2}\sigma_e\big|_{i,j',k'}\left(E_x\big|^{n-1/2}_{i,j',k'} + E_x\big|^{n+1/2}_{i,j',k'}\right), \end{aligned} \tag{3}$$

$$\begin{aligned} \frac{B_x\big|^{n+1}_{i',j'',k''} - B_x\big|^{n}_{i',j'',k''}}{\Delta t} = \frac{E_y\big|^{n+1/2}_{i',j'',k'''} - E_y\big|^{n+1/2}_{i',j'',k'}}{\Delta z} - \frac{E_z\big|^{n+1/2}_{i',j''',k''} - E_z\big|^{n+1/2}_{i',j',k''}}{\Delta y} - \\ M_x\big|^{n+1/2}_{i',j'',k''} - \frac{1}{2}\sigma_m\big|_{i',j'',k''}\left(H_x\big|^{n}_{i',j'',k''} + H_x\big|^{n+1}_{i',j'',k''}\right). \end{aligned} \tag{4}$$

Here $j' = j + 1/2$, $j'' = j + 1$, $j''' = j + 3/2$ and similarly for other subscripts. Numerical approximations of remaining Maxwell's equations can be obtained from (3,4) by a cyclic permutation of x, y, z and the corresponding change in subscripts.

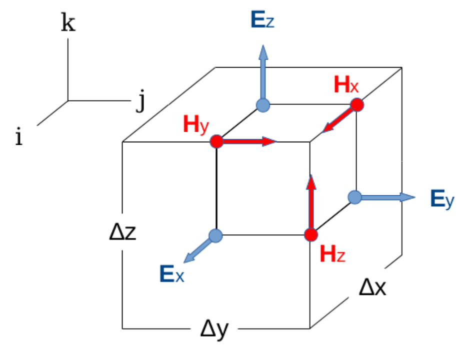

Fig. 1. *FDTD computational stencil*

The distributions of **J** and **M** are specified in such a way as to generate the incident electromagnetic wave or beam interacting with a material medium within the computational domain. In order to avoid or minimize false numerical reflections of scattered waves from boundaries of the computational domain, the perfectly matched layer (PML) technique [3, 4] is employed. The computational domain is surrounded by a buffer zone filled with an artificial uniaxial anisotropic (with diagonal tensors $\bar{\bar{\epsilon}}$ and $\bar{\bar{\mu}}$) medium whose electric and magnetic conductivities grow rapidly with the distance from the computational domain boundary so that electromagnetic waves are absorbed virtually with no reflection.

In all cases considered below the medium is either anisotropic with a non-diagonal tensor $\bar{\bar{\epsilon}}$ but non-conductive or conductive but isotropic. So the FDTD scheme is only diagonally implicit and the solution on a new time level can be calculated non-iteratively. If the tensor $\bar{\bar{\epsilon}}$ is non-diagonal then, in order to calculate the electrical field **E**, all three components of **D** should be known in the same point that is not the case with the FDTD staggered grid. Thus, two missing components are determined by averaging over 4 neighboring grid nodes. More details about the FDTD method for anisotropic media can be found in [5].

Numerical simulations have been performed on the computational cluster of Novosibirsk State University. The code is written in Fortran-90 and parallelized using MPI. The computational domain is divided into rectangular blocks by planes parallel to the coordinate planes. Each block is assigned to one computational core. The domain decomposition in all three dimensions allows one to decrease the data transfer between processors in comparison with 1D or 2D decomposition. Tests performed on a grid containing $8 \cdot 10^6$ cells have shown that the computation with 16 cores is approximately 11 times faster than with a single core so that the efficiency of parallelization is close to 70%, see Fig. 2.

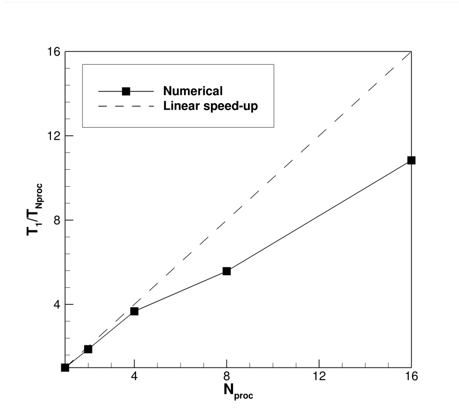

Fig. 2. *Numerical speed-up*

In different simulations presented below, spatial resolution was from 10 up 30 grid cells per a wavelength. Typically, a grid block assigned to each processor core consisted of $150^3 = 3.375 \cdot 10^6$ cells. The largest grid used contained $6{\cdot}10^8$ cells, 180 cores were employed to perform numerical simulation on this grid.

3 Laser drilling

Today lasers are successfully applied for cutting, welding and drilling of materials [6, 7]. Nevertheless, the problem of prediction of laser energy distribution over the cut surface is still of current interest because of the appearance of new materials and sources of laser radiation as well as growing requirements to the quality of laser treatment of materials.

Usually this problem is solved using geometrical optics approximation: the laser beam is represented as a set of single light rays, which are reflected and refracted on the metal surface according to Fresnel's laws [8, 9]. However, in many cases it is not correct because small features of the treated surface can be comparable in size with the radiation wavelength. Below we compare results obtained using wave and geometrical optics approaches.

The problem under consideration is illustrated in Fig. 3a. A Gaussian beam of circularly polarized electromagnetic radiation propagates along the z axis. A cavity in a metal model is aligned coaxially with the beam. The cavity surface shape is specified analytically. The problem formulation corresponds to an initial stage of a laser drilling process. It is required to determine electromagnetic fields and calculate the volumetric density of absorbed radiation w in the metal surrounding the cavity surface. This density is equal to the time-averaged value of the divergence of the Poynting vector (with the opposite sign):

$$w = -\langle \nabla \cdot \mathbf{P} \rangle = -\nabla \cdot \langle \mathbf{E} \times \mathbf{H} \rangle . \quad (5)$$

Further, the dependence of absorbed energy on the cavity depth can be calculated as an integral of the volumetric density over the azimuthal angle and the distance from the axis.

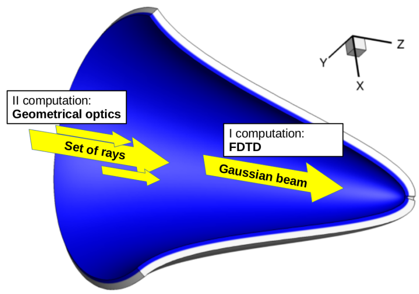

a)

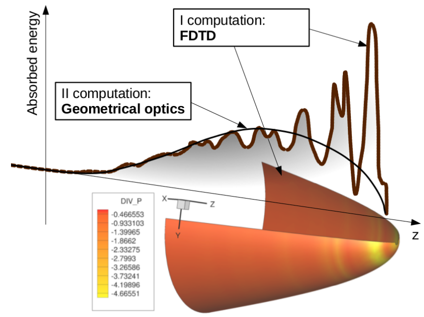

b)

Fig. 3. *Schematic of laser drilling problem (a) and distribution of the absorbed power (b): I — FDTD simulations, II — ray optics calculations*

The FDTD simulations were performed on the computational grid containing $16 \cdot 10^6$ cells with 10 Gb of RAM and 16 processors used.

Figure 3b demonstrates a substantial qualitative difference of results obtained by solving Maxwell's equations and with geometrical optics approximation in a situation when the channel sizes are comparable with the wavelength. Additionally, the results of FDTD simulations point out that one possible reason for deterioration of laser drilling quality is a annular corrugation of the cavity bottom caused by nonuniform heating or vortex formation in the gas stream flowing over the region of melting.

More details about the results of numerical simulations of the laser drilling process can be found in [10].

4 Fiber-coupled liquid crystal system

Liquid crystals (LC) is one of well-known examples of soft matter materials. Their unique optical properties are widely used in many devices. Along with other remarkable properties, they also have anomalously high values of nonlinear susceptibilities. In particular, the light-induced quadratic optical nonlinearity with a susceptibility index is several orders of magnitude higher than in solid crystals was observed in LCs experimentally [11].

The utilization of LCs as an active element of laser systems was reviewed in [12]. A very high efficiency allows LCs to be used in microscopic volumes for conversion and control of coherent radiation [13].

Recently a research team from Institute of Laser Physics (Novosibirsk, Russia), Novosibirsk State University and Aston Institute of Photon Technologies

(UK) proposed to use a microscopic (2–8 μm) LC system placed inside the optical fiber as an optical trigger and a converter of electromagnetic radiation [14, 15].

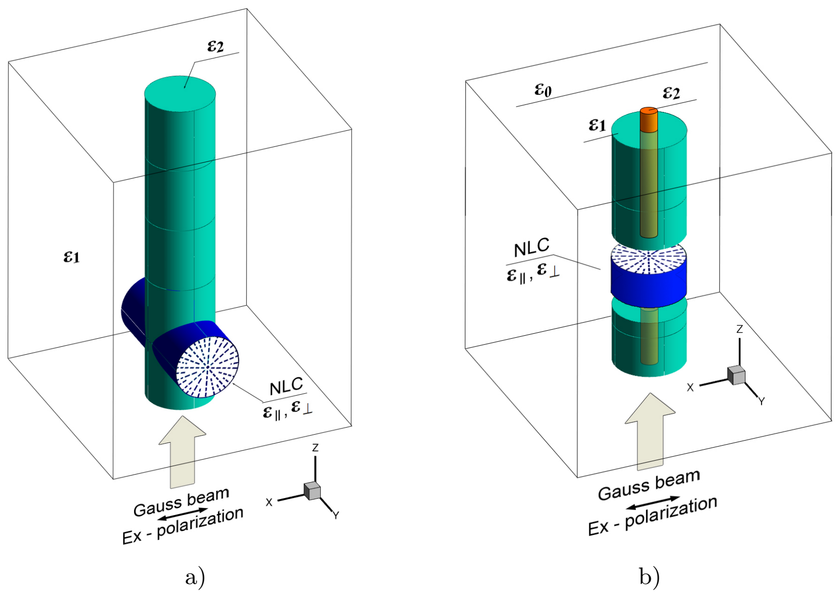

Fig. 4. *Two configurations of fiber-coupled LC system: with cylindrical cavity filled with LC (a) and with plane layer of LC (b)*

In the present paper the proposed integrated optical system is simulated numerically and the effects of cavity shape on light propagation are investigated. We simulate the interaction of a Gaussian laser beam propagating in the optical fiber with a nematic LC which fills a cavity whose size is comparable with the laser radiation wavelength. The laser beam is plane polarized.

Numerical simulations are performed for two different configurations of the proposed system (see Fig. 4). In the first case, the cavity is a cylindrical hole drilled across the optical fiber core. In the second case, the fiber is cut across and a plane layer of LC fills the gap formed. The first configuration is close to that was investigated in the experiment [14], the second — in the experiment [15]. The direction of preferred orientation of molecules at any point of LC is represented by a unit vector **n**, the director. In both the cases it is supposed that the director distribution is radially aligned and contains a linear singularity, the disclination of strength +1 [16], in the center. In the first case, the disclination coincides with the axis of the cylindrical hole, in the second case — with the axis of the optical fiber. In the experiments, the director alignment is forced using specially treated solid walls bounding the LC volume or by imposing an external heat flux.

The dielectric permittivity tensor for a LC medium is

$$\bar{\bar{\epsilon}} = \{\epsilon_{\alpha\beta}\} = \epsilon_{\perp}\delta_{\alpha\beta} + \left(\epsilon_{\parallel} - \epsilon_{\perp}\right) n_{\alpha} n_{\beta}, \tag{6}$$

where $\epsilon_{\parallel} = 2.82$ and $\epsilon_{\perp} = 2.28$ are the permittivities parallel and perpendicular to the director, $\delta_{\alpha\beta}$ is the Kronecker delta.

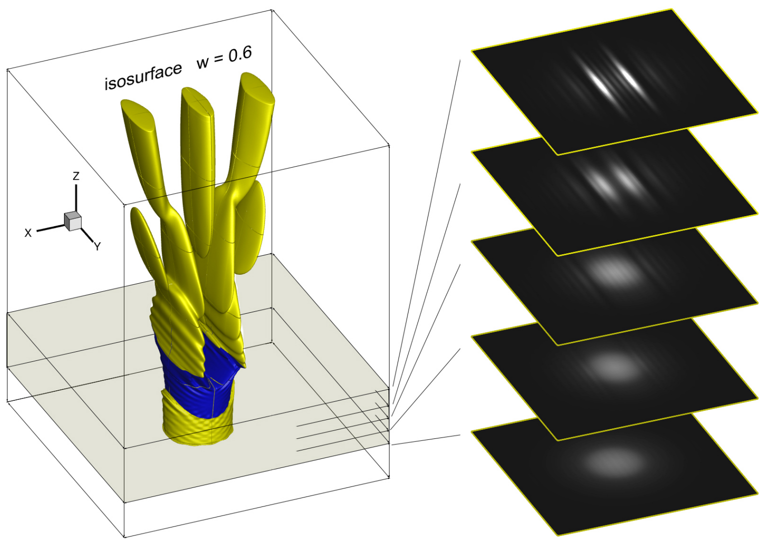

a) b)

Fig. 5. *Energy density of electromagnetic field: isosurface (a) and surface distributions in 5 successive cross-sections (b)*

Numerical simulations for the first configuration (Fig. 4a) were performed on the grid of $27 \cdot 10^7$ cells using 80 processors and 80 Gb of RAM in total. They allows us to study how the intensity and directivity of laser beam change as a result of interaction with the transverse cylindrical cavity filled with a LC. Figure 5 shows the spatial distribution of energy density of electromagnetic field. It can be concluded that this configuration has serious drawbacks: the radiation is focused behind the cavity so that the optical fiber can burn out at high powers of the laser pulse, in addition a significant portion of the radiation is scattered outside the fiber core.

Numerical simulations for the second configuration when the laser beam passes through a layer of the LC filling a gap in a optical fiber (Fig. 4b) were performed on the grid of $48.5 \cdot 10^7$ cells using 144 processors and 145 Gb of RAM in total. A series of simulations with different values of the gap width h were conducted. In contrast to the first configuration, no significant scattering

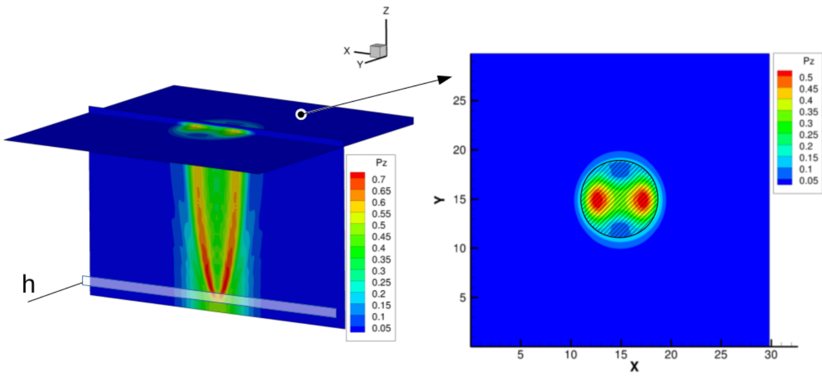

Fig. 6. *Distributions of z-component of energy flux density in three different cross-sections*

of radiation was observed (Fig. 6). The dependence of the reflection coefficient (the portion of energy reflected backwards) on the gap width is not monotonous having maximums and minimums at certain values of h. It can be explained by interference: the system behaves similar to a resonator with losses.

Thus, the configuration in which the laser beam passes through a plane layer of a LC material is preferable in comparison with that include a transverse cylindrical hole.

It is worth noting that in the present paper we neglect the influence of electromagnetic radiation on the properties of the medium so that the main subject of investigation is transformation of a laser beam in a non-homogeneous and anisotropic medium. A similar approach was used in many works on computational photonics, in particular devoted to electrodynamics of metamaterials — see, e.g., the recent paper [17] whose main subject is close to that of our investigation. It is clear that such approach is correct if the intensity of radiation is not very high so that one can neglect nonlinear effects.

5 Generation of twisted optical beams

Generation, investigation and utilization of "optical vortices", i.e. light beams with helical dislocations of the wave front, is one of most rapidly developing area of modern optics [18]. Such "twisted" beams have not only the spin angular moment of photons but also an orbital angular momentum. Optical vortices find applications in many areas, from microscopy and manipulation of microscopic objects up to improvement of communication bandwidth and processing of images of astronomical objects [19, 20].

Optical vortices can be effectively generated at the interaction of light with LCs. The advantage of this approach is the possibility to change the parameters of the output beam dynamically using weak external electromagnetic fields or mechanical and thermal stresses applied to the LC [21].

We performed numerical simulations of generation of optical vortices at propagation of a laser beam through a plane layer of nematic LC located in a gap between two ends of an optical fiber (Fig. 7). The laser beam propagating in the optical fiber represented the eigenmode HE_{11}. There was a disclination in the director distribution within the LC, which coincided with the fiber axis. The influence of the disclnation strength s and the gap width Δh on the angular moment of the transmitted beam was been investigated. The computational domain was meshed with a grid containing $6 \cdot 10^8$ cells, 180 processors and 185 Gb of RAM were used for the computation.

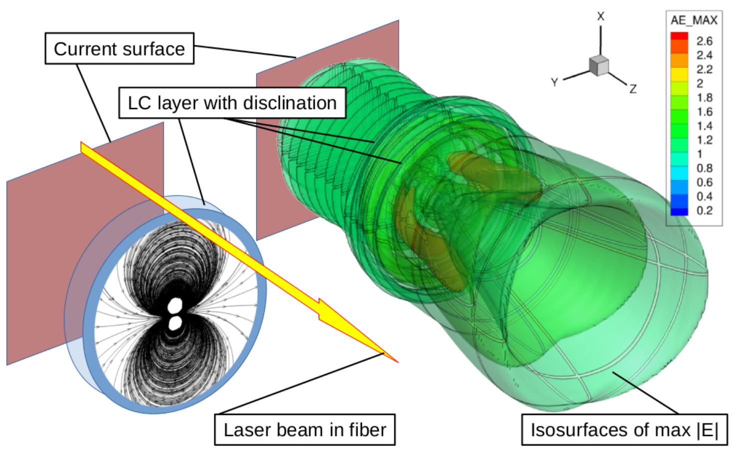

Fig. 7. *Optical vortex generation at interaction of laser beam with LC. The disclination strength* $s = 2$

A general view of laser beam transformation is shown in Fig. 7 where isosurfaces of the maximum intensity of electric field are displayed. In the region ahead of the nematic LC layer the isosurfaces are corrugated because of the interference of incident and reflected beams. The interaction with a birefringent non-homogeneous medium leads to an extension of the beam and transferred an additional angular momentum to it.

The efficiency of angular momentum transfer can be characterized by the ratio of angular momentum of the transmitted beam (calculated with respect to the beam axis) to the energy flux:

$$LP_z(z) = \iint\limits_{-\infty}^{+\infty} \left[xP_y(x,y,z) - yP_x(x,y,z)\right] dxdy \Bigg/ \lambda \iint\limits_{-\infty}^{+\infty} P_z(x,y,z)dxdy. \quad (7)$$

Here P_x, P_y, P_z are the components of the time-averaged Poynting vector, λ is the wavelength of incoming radiation.

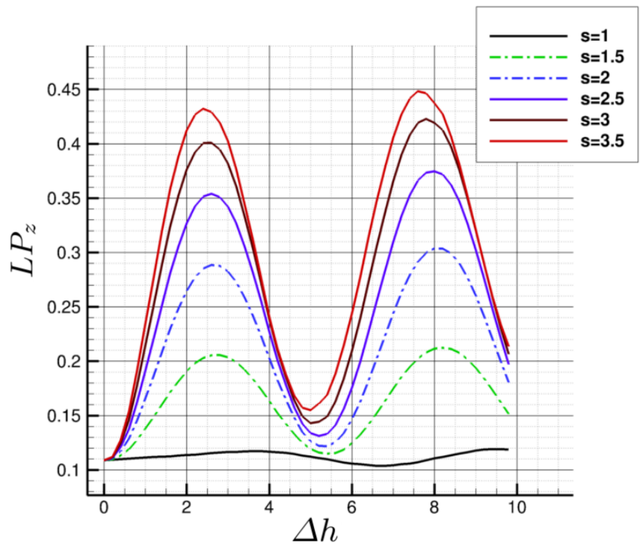

Fig. 8. *Dependence of LP_z on the gap width at different disclination strengths*

The dependence of LP_z on the gap width for different strengths of the disclination is shown in Fig. 8. The non-monotonic, quasi-periodic behavior of $LP_z(z)$ deserves special attention: the beam is twisted and untwisted periodically. At the first glance, if light is twisted in a thin LC layer then an increase in the layer thickness should increase the twist. However, computations show that such conclusion is erroneous and the transferred angular momentum varies periodically with the gap width.

6 Conclusion

Numerical simulations of the interaction of electromagnetic radiation with a number of composite and anisotropic media were performed using supercomputers. The processes of laser treatment of materials such as laser drilling were simulated. It was demonstrated that, in many practical cases, the geometrical optics approximation (ray optics) is not sufficient for correct evaluation of the absorbed energy distribution, the latter can be achieved only by solving the full Maxwell's equations.

A fiber-coupled LC systems, which can be recently proposed for employing as an optical trigger and a converter of electromagnetic radiation, were simulated in two different configurations. It was shown that one of these configurations, containing a transverse cylindrical hole filled with a nematic LC, is impractical because of scattering of a significant portion of radiation outside the fiber core and focusing of another portion that can cause damage to the fiber. At the same time, the second configuration, in which the light beam passes through a LC layer, enable us to preserve most of radiation inside the fiber core and, thus, appears more suitable for a practical use.

The generation of light beams possessing an orbital angular momentum at propagation of laser radiation through a layer of a nematic LC containing disclinations of different strengths in the director field distribution was investigated numerically. It was found that the generated angular momentum grows as the disclination strength increases. A periodic dependence of the generated angular momentum on the layer thickness was observed that can be used to determine the optimal parameters for generation of such "twisted" beams.

7 Acknowledgements

This work was supported by Russian Foundation for Basic Research (joint Russia-India project No. 16-57-48007). Computational resources were kindly provided by Computational Center of Novosibirsk State University (nusc.nsu.ru).

References

1. Yee, K.S.: Numerical solution of initial boundary value problems involving Maxwell's equations in isotropic media. IEEE Trans. Antennas Propag., 14, 302–307 (1966)
2. Taflove, A., Hagness, S.C.: Computational Electrodynamics, 3rd ed. Artech House, Boston & London (2005)
3. Berenger J.-P.: Three-dimensional perfectly matched layer for absorption of electromagnetic waves. J. Comput. Phys., 127, 363–379 (1996)
4. Berenger J.-P.: Perfectly Matched Layer (PML) for Computational Electromagnetics. Morgan & Claypool (2007)
5. Schneider J., Hudson S.: The finite-difference time-domain method applied to anisotropic material. IEEE Trans. Antennas Propag., 41, 994–999 (1993)
6. Steen W.M., Mazumder J.: Laser Material Processing, 4th ed. Springer, London (2010)
7. Gladush G.G., Smurov I.: Physics of Laser Materials Processing: Theory and Experiment. Springer, Berlin (2011)
8. Duan J., Man H.C., Yue T.M.: Modeling the laser fusion cutting process. I. Mathematical modeling of the cut kerf geometry for laser fusion cutting of thick metal. J. Phys. D. Appl. Phys., 34, 2127-2134 (2001)
9. Kovalev O.B., Zaitsev A.V.: Modeling of the free-surface shape in laser cutting of metals. 2. model of multiple reflection and absorption of radiation. J. Appl. Mech. Tech. Phys., 46, 9–13 (2005)
10. Kovalev O.B., Galjov R.V.: The application of Maxwell's equations for numerical simulation of processes during laser treatment of materials. J. Phys. D: Appl. Phys., 48, 1–12 (2015)

11. Trashkeev S.I., Klementyev V.M., Pozdnyakov G.A.: Highly efficient lasing at difference frequencies in a nematic liquid crystal. Quantum Electronics, 38, 373–376 (2008)
12. Coles H., Morris S.: Liquid-crystal lasers. Nature Photonics, 4, 676–685 (2010)
13. Nyushkov B.N., Trashkeev S.I., Klementyev V.M., Pivtsov V.S., Kobtsev S.M.: Generation of harmonics and supercontinuum in nematic liquid crystals. Quantum Electronics, 43, 107–113 (2013).
14. Nyushkov B.N., Pivtsov V.S., Trashkeev S.I., Denisov V.I., Bagayev S.N.: Fiber laser systems for applied metrology and photonics. In: Russian-Chinese Workshop on Laser Physics and Photonics (Novosibirsk, Russia, August 26-30, 2015). Tech. digest, pp. 69-70 (2015)
15. Trashkeev S.I., Nyushkov B.N., Galev R.V., Kolker D.B., Denisov V.I. Optical trigger based on a fiber-coupled liquid crystal. In: 17-th International Conference "Laser Optics 2016" (St. Petersburg, Russia, 27 June - 1 July, 2016). Tech. digest, pp. 69–70 (2016)
16. De Gennes P.G., Prost J.: The Physics of Liquid Crystals, 2nd ed. Oxford, Clarendon Press (1993)
17. Čančula M., Ravnik M.,Žumer S.: Generation of vector beams with liquid crystal disclination lines. Phys. Rev. E, 90, 022503 (2014).
18. Franke-Arnold S., Allen L., Padgett M.: Advances in optical angular momentum. Laser & Photon Rev., 2, 299–313 (2008)
19. Yao A. M., Padgett M. J.: Orbital angular momentum: origins, behavior and applications. Adv. Opt. Photon. 3, 161–204 (2011).
20. Ritsch-Marte M.: Orbital angular momentum light in microscopy. Phil. Trans. R. Soc. A 375, 20150437 (2017)
21. Karimi E., Piccirillo B., Nagali E., Marrucci L., Santamato E.: Efficient generation and sorting of orbital angular momentum eigenmodes of light by thermally tuned q-plates. Appl. Phys. Lett., 94, 231124 (2009).